# Thermal Rate Constants of the NO$_2$ Fission Reaction of Gas Phase α-HMX: A Direct ab Initio Dynamics Study

### Shaowen Zhang and Thanh N. Truong*

*Henry Eyring Center for Theoretical Chemistry, Department of Chemistry, University of Utah, 315 South 1400 E, Room 2020, Salt Lake City, Utah 84112*

The NO$_2$ fission reaction of gas phase α-HMX has been studied using a direct ab initio method within the framework of microcanonical variational transition state theory ($\mu$VT). The potential energy calculations were calculated using the hybrid nonlocal B3LYP density functional theory with the cc-pVDZ basis set. The calculated results show that the potential energy of breaking the axial NO$_2$ groups is lower than that of breaking the equatorial NO$_2$ groups. No traditional transition state was found along the reaction path. Microcanonical rate constants calculation shows the variational transition state varies from 2.0 to 3.5 Å of the breaking N−N bond length as a function of the excess energy. The $\mu$VT method was used for thermal rate constants calculation over a temperature range from 250 to 2000 K. The fitted Arrhenius expression from the calculated data is $k(T) = 1.66 \times 10^{15} \exp(-18748\text{K}/T)$ s$^{-1}$, which is in good agreement with the experimental data at low temperatures.

## Introduction

HMX (octahydro-1,3,5,7-tetranitro-1,3,5,7-tetrazocine) is one of the most important energetic nitramines which are used as explosives and propellants. The decomposition of HMX is quite complicated and involves hundreds of elementary reactions.[1] It has been recognized that NO$_2$ fission is one of the most important initial reactions in the thermal decomposition of nitramines.[2−5] Many experimental studies have focused on the kinetics of this reaction.[2,3] However, since HMX is explosive at higher temperatures, the experiments were often carried out at relatively lower temperatures ($T < 400$ K). Furthermore, since the measurement of rate constants were affected by several factors such as molecular clustering and secondary reactions, the observed Arrhenius activation energies $E_a$ and thermal rate constants are quite scattered.[6] Because the NO$_2$ fission reaction plays an important role in the decomposition of HMX, theoretical study on both the energetic and the dynamics of this reaction is necessary.

HMX has four crystalline polymorphs, namely α, $\beta$, $\gamma$ and $\delta$, among which α, $\gamma$ and $\delta$ polymorphs have similar conformations which are different from the conformation of $\beta$ polymorph.[7] Several theoretical studies have performed on the structure of HMX.[8−10] A most recent study by Smith and Bharadwaj investigated the conformations of HMX at B3LYP/6-311G** level of theory.[7] They found the energies of α form and $\beta$ form are close.

To the best of our knowledge, there is no theoretical study on the dynamics of the NO$_2$ fission reaction of HMX. However, there were several studies on the dynamics of similar reactions of small molecules and of RDX (1,3,5-trinitro-hexahydro-s-triazine).[1,11,12] Especially, detailed studies on the NO$_2$ fission of dimethylnitramine showed that the calculated geometries and energies at the B3LYP/cc-pVDZ level of theory are quite close to those calculated at QCISD/cc-pVDZ level of theory.[12]

In the present study, we employed the direct ab initio dynamics method[13,14] developed in our laboratory to calculate the thermal rate constants for the NO$_2$ fission reaction of the α form of HMX (denoted as α-HMX). Rate calculations are done using our recent implementation of the microcanonical variational transition state theory ($\mu$VT).[15]

## Methodology

**I. Microcanonical Variational Transition State Theory.** The thermal rate constant at a fixed temperature $T$ within the framework of $\mu$VT is given by[16,17]

$$k^{\mu\text{VT}}(T) = \sigma \frac{\int_0^\infty \min_s\{N^{\text{GTS}}(E,s)\}\mathrm{e}^{-E/k_\text{B}T}\,\mathrm{d}E}{hQ_R} \qquad (1)$$

where $\sigma$ is the statistical factor of the reaction as discussed below to have the value of 4 for this reaction; $h$ and $k_B$ are the Planck's and Boltzman's constants, respectively. $Q_R$ is the total partition function of the reactant. $\min_s\{N^{\text{GTS}}(E,s)\}$ is the minimum of the sum of states of the generalized transition state locating at $s$ at energy $E$ along the minimum energy path (MEP). $s$ is the reaction coordinate. The relative translational partition function was calculated classically and was included in $Q_R$. However, the rotational and vibrational degrees of freedom of the reactant and the generalized transition states were treated quantum mechanically within the rigid rotor and harmonic oscillator approximation.

The rate constants calculations were carried out employing the TheRate program.[14]

**II. Electronic Structure Calculations.** Earlier studies have shown that the hybrid density function theory can give good prediction of the potential energy information along the MEP.[18] In this study, all the calculations were carried out using the hybrid nonlocal density functional theory B3LYP with the Dunning's correlation-consistent double-$\zeta$ basis set (cc-pVDZ). The NO$_2$ fission reaction of HMX generates two free radicals; thus, the singlet open shell B3LYP method with a mix of the frontier molecular orbitals was adopted in all the calculations.
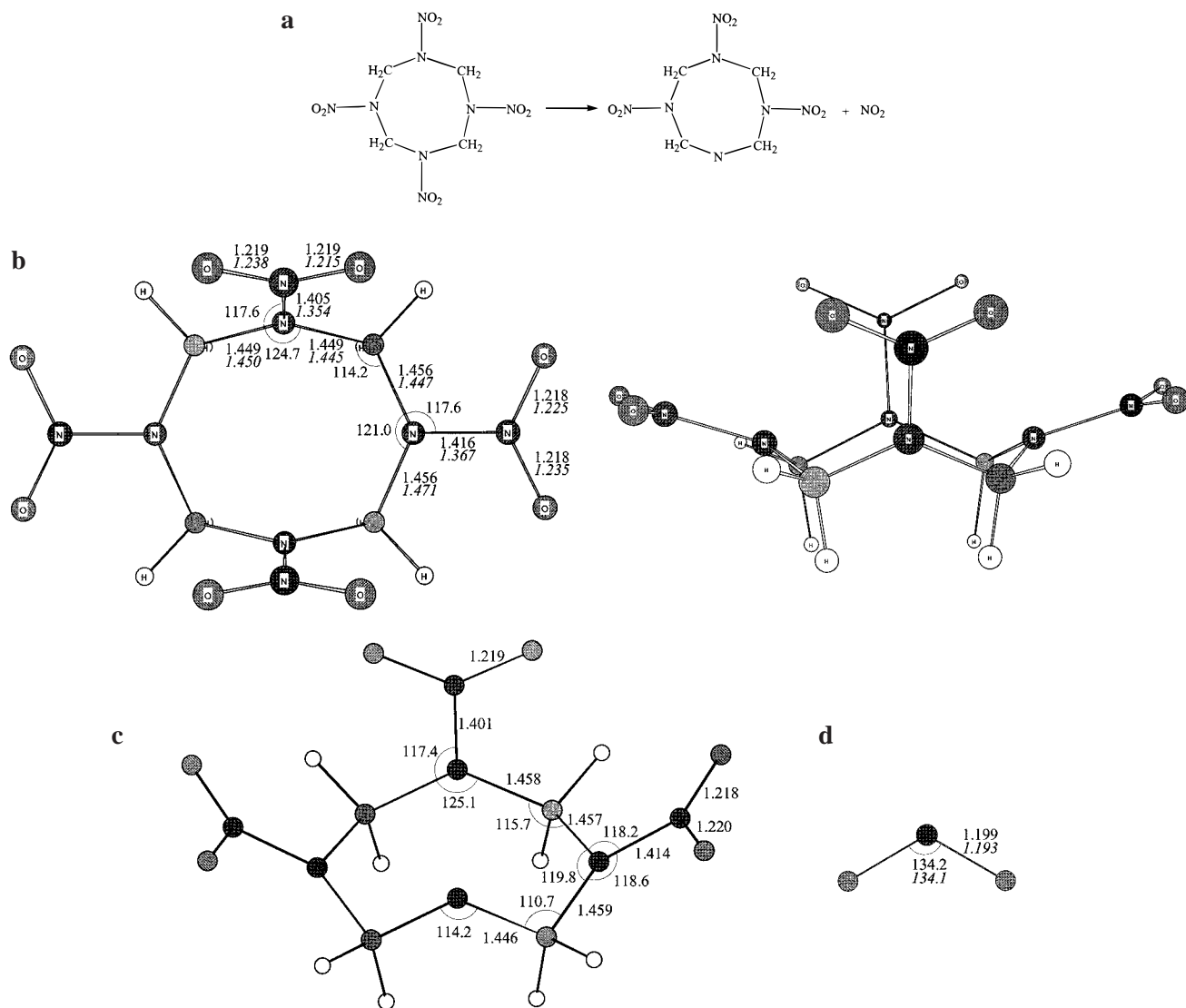
NO₂ Fission Reaction of Gas Phase α-HMX

*J. Phys. Chem. A, Vol. 104, No. 31, 2000* **7305**



**Figure 1.** Schematic diagram of the NO₂ fission reaction of α-HMX (a) and the optimized structures of α-HMX (b), HMX-dNO₂ (c), and NO₂ (d) at B3LYP/cc-pVDZ level of theory. The *italic* numbers are experimental data taken from refs 18 and 19 for α-HMX and NO₂, respectively. The atom types are indicated in α-HMX (a).

The distance of the broken N–N bond was selected as the reaction coordinate since no barrier was found along the reaction path. At a given value of the reaction coordinate, all remaining parameters are fully optimized. The Hessian matrix of each point was calculated and used to calculate the rate constants. All electronic structure calculations were performed using the GAUSSIAN 98 program.[19]

## Results and Discussion

**I. Equilibrium Structures.** A schematic diagram of the NO₂ fission reaction of α-HMX and the optimized structures of α-HMX, NO₂ and HMX-dNO₂ (HMX after the loss of a NO₂) are depicted in Figure 1. The symmetry of the optimized structure of α-HMX is $C_{2v}$, which is a little different from the $C_2$ symmetry predicted by experiment.[20] The reason for this is that the optimization is performed in an isolated condition, whereas the experimental X-ray structure was affected by the crystal environment. In our previous study, we found that crystal polarization is large and thus may have an effect on the crystal structure.[21] From Figure 1 we can see the largest differences of bond lengths between the calculation and experiment is the N–N bond length, with the calculated values are generally 0.05 Å

larger than the experimental results. The differences of N–C and N–O bond lengths between the calculation and experiment are smaller than 0.019 Å. These differences are not large, indicating the gas-phase structure of α-HMX may be close to that of solid phase. The optimized structure of HMX-dNO₂ has $C_s$ symmetry. The bond lengths of HMX-dNO₂ are close to the corresponding ones of α-HMX. The largest difference between both structures is the N–C bonds opposite to the leaving NO₂ group, which is about 0.009 Å longer in HMX-dNO₂ than that in α-HMX. The differences of other bond lengths between α-HMX and HMX-dNO₂ are smaller than 0.003 Å. The bond angles of α-HMX are also close to that of HMX-dNO₂ with the largest difference smaller than 1.5° except the C–N–C and N–C–N angles near the breaking NO₂, which are 10.5° and 3.5° larger than those of HMX-dNO₂. The change of bond angles is due to the change of hybridization from sp² to sp³ of the nitrogen atom that connects to the breaking NO₂. We calculated the relaxation energy (energy of optimized HMX-dNO₂ − energy of HMX-dNO₂ at the α-HMX geometry) to be 9.19 kcal/mol. The optimized geometry of NO₂ is in good agreement with experimental results; the calculated N–O bond

**TABLE 1:  Calculated Frequencies of α-HMX, HMX-dNO₂ and NO₂**

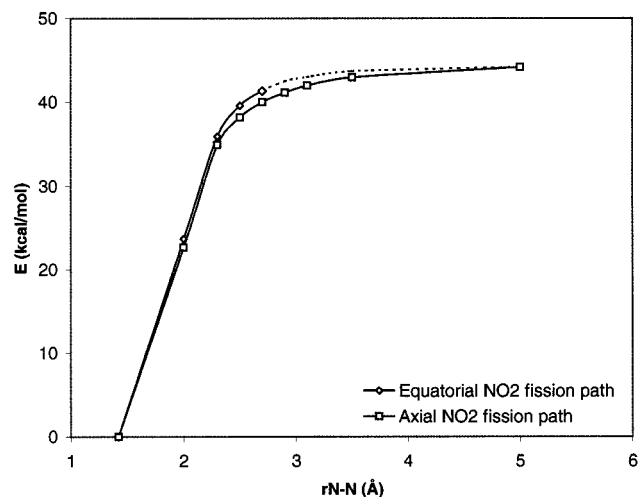| | frequencies (cm⁻¹) | | | | | | | | | | |
|---|---|---|---|---|---|---|---|---|---|---|---|
| α-HMX | 29 | 47 | 53 | 54 | 68 | 96 | 100 | 102 | 104 | 135 | 188 | 194 |
| | 214 | 262 | 327 | 364 | 386 | 401 | 408 | 412 | 442 | 463 | 586 | 596 |
| | 624 | 641 | 646 | 647 | 721 | 744 | 763 | 763 | 772 | 777 | 850 | 859 |
| | 884 | 889 | 900 | 928 | 929 | 929 | 1016 | 1086 | 1116 | 1191 | 1243 | 1246 |
| | 1277 | 1289 | 1305 | 1308 | 1330 | 1346 | 1358 | 1362 | 1373 | 1397 | 1398 | 1399 |
| | 1413 | 1418 | 1440 | 1441 | 1447 | 1455 | 1671 | 1691 | 1694 | 1701 | 3033 | 3033 |
| | 3042 | 3046 | 3182 | 3183 | 3184 | 3185 | | | | | | |
| HMX-dNO₂ | 45 | 54 | 59 | 73 | 99 | 121 | 128 | 186 | 191 | 224 | 243 | 326 |
| | 362 | 364 | 397 | 418 | 437 | 447 | 475 | 596 | 612 | 623 | 633 | 718 |
| | 727 | 760 | 761 | 775 | 852 | 862 | 876 | 911 | 913 | 929 | 941 | 982 |
| | 1076 | 1087 | 1133 | 1179 | 1192 | 1238 | 1268 | 1283 | 1301 | 1314 | 1317 | 1350 |
| | 1352 | 1373 | 1376 | 1390 | 1396 | 1416 | 1418 | 1435 | 1446 | 1454 | 1675 | 1687 |
| | 1697 | 2953 | 2957 | 3069 | 3081 | 3104 | 3109 | 3176 | 3178 | | | |
| NO₂ | 757 (750ᵃ) | 1406 (1318) | 1722 (1696) | | | | | | | | | |

*ᵃ* Experimental data, take from ref 22.



**Figure 2.** Plot of potential energy profile vs the breaking N−N bond length for the axial NO₂ fission and equatorial NO₂ fission reactions. The dashed line means the structures in this region of equatorial NO₂ fission converge to the same structures of axial NO₂ fission mechanism.



**Figure 3.** Plot of $\log[k(E)]$ vs the breaking N−N bond length at different excess energies.

lengths and O−N−O bond angle are 0.006 Å and 0.1° larger than the experimental ones, respectively.

Table 1 lists calculated frequencies and available experimental data.[22] The computed frequencies for NO₂ are ∼0.9−6.7% larger than the experimental harmonic frequencies. There are some low-frequency floppy vibration modes for α-HMX and HMX-dNO₂. The anharmonicity effects may be noticeable for these modes. Howerver, inclusion of anharmonicity effects involves third-order derivatives and thus is computationally quite demanding particularly for variational μVT calculations.

**II. Reaction Path.** The HMX → NO₂ + HMX-dNO₂ reaction is found to be an endothermic process without a barrier at the B3LYP/cc-pVDZ level of theory. Since the geometries of α-HMX and HMX-dNO₂ are quite similar as mentioned above, one can expect the reaction coordinate consists of mainly motion of the N−N bond. Thus, we can use the distance of the breaking N−N bond as an approximation of the reaction coordinate for the N−N bond fission reaction. The variation of energy with reaction coordinate is shown in Figure 2. α-HMX has two types of NO₂ group, one is axial NO₂ and the other is equatorial NO₂. We calculated the dissociation reaction paths for both types of NO₂ groups. Both dissociation paths differ slightly by at most 1.4 kcal/mol in the reactive region ($r = 2.3-2.7$ Å) and become degenerate in the exit channel. For this reason, we use the reaction symmetry number of 4 to account for dissociation from both paths. The actual rate constants should be somewhat smaller
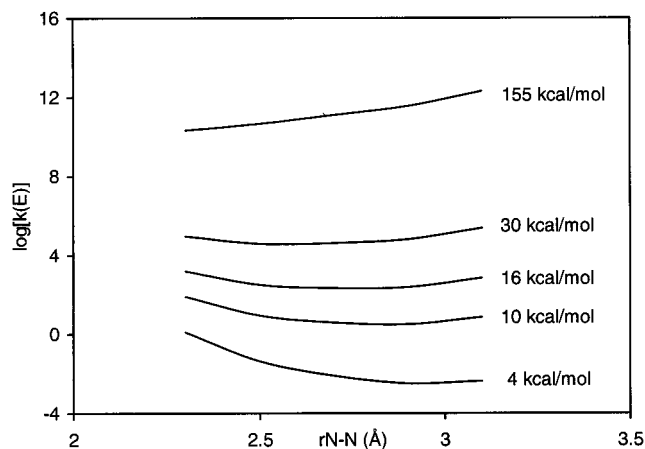
due to the smaller contributions of the higher-energy path. The calculated reaction energy is 44.17 kcal/mol, which is slightly smaller than the estimated N−N bond breaking energies (48 kcal/mol) of α-HMX by Melius.[1] However, the calculated reaction energy decreased to 39.73 kcal/mol if the vibrational zero-point energies are included. The potential energy profile becomes flat as the breaking N−N bond length is larger than 2.5 Å; i.e., the energy rises only 3.79 kcal/mol in the range from 2.5 to 3.5 Å. As shown below, this region is important for the variational transition state calculations.

**III. Rate Constants.** Figure 3 shows the plot of microcanonical rate constants $k(E)$ vs the N−N bond length at different excess energies. It is clear that the dynamical bottleneck, i.e., the microcanonical variational transition state (minimum of $k(E)$, μVTS) shifts closer to the exit channel as the excess energy decrease. At the excess energy of 155 kcal/mol, the μVTS appears at $R_{N-N}$ about 2.3 Å. When the excess nergy lowers to 4 kcal/mol, the μVTS shifts to 3.0 Å. Thus, a microcanonical variational treatment is necessary for calculating the thermal rate constants of this reaction.

The microcanonical variational transition state theory (μVT) was employed to calculate the thermal rate constants of the NO₂ fission reaction in the temperature range from 250 to 2000 K. The range of the reaction coordinate between 2.0 and 3.5 Å is sufficient to treat variational effects in this temperature range. The calculated rate constants are displayed in Figure 4 along with experimental data[2−5] and RRKM estimation for the NO₂ fission reaction of RDX.[1] The RRKM prediction for RDX has been used to model the kinetics of thermal decomposition of HMX. It can be seen from Figure 4 that the rate constants for
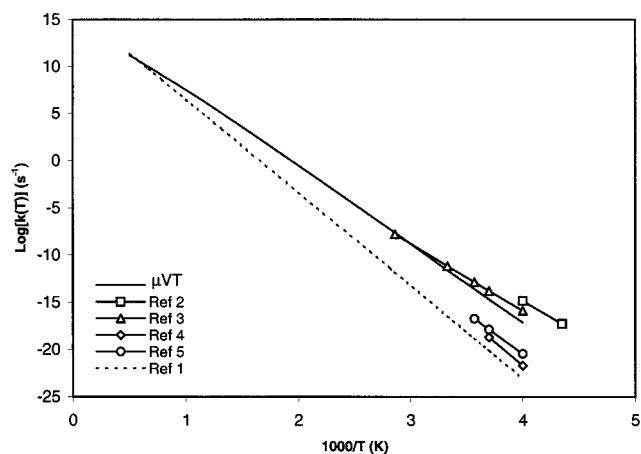
NO$_2$ Fission Reaction of Gas Phase α-HMX

*J. Phys. Chem. A, Vol. 104, No. 31, 2000* **7307**



**Figure 4.** Comparison of the calculated and experimental log[$k(T)$] vs 1000/$T$. The dotted line is calculated from the Arrhenius expression taken from Melius' RRKM results for RDX (ref 1).

the NO$_2$ fission reactions of both RDX and HMX are close at high temperatures (1000−2000 K), but they differ significantly at low temperatures. Because of the difficulties in experimental measurement, the experimental data are only available for temperatures below 400 K and are scattered with the largest difference of log $k(T)$ of 5.6 at 250 K. In the temperature range 250−400 K, the calculated results are located within the experimental uncertainty. However, the differences between the experimental and calculated data become smaller as the temperature increase. The fitted Arrhenius expression from the calculated data is $k(T) = 1.66 \times 10^{15} \exp(-18748K/T)$ s$^{-1}$. The fitted activation energy is 37.25 kcal/mol, which is 2.5 kcal/mol smaller than the zero-point energy corrected reaction energy. This value is close to the measured Arrhenius activation energies of Burov et al.[5] (39.6 kcal/mol) and Maksimov et al.[4] (38 ± 2.8 kcal/mol). Since experimental measurement of the NO$_2$ fission reaction of α-HMX is rather difficult at high temperatures, the calculated rate constants in present work can provide useful information for modeling the thermal decomposition of α-HMX.

## Conclusion

We have presented in this work a direct ab initio study on the mechanism and dynamics of the NO$_2$ fission reaction of α-HMX. Microcanonical rate constants calculations show that the variational transition state is located between 2.0 and 3.5 Å. Microcanonical variational transition state theory was further employed for calculating the thermal rate constants in a wide temperature range of 250−2000 K. The predicted rate constants are in agreement with the available experimental data at low temperatures and they provide reference to the high-temperature rate constants. The fitted Arrhenius equation of the calculated rate constants over the temperature range 250−2000K can be expressed as $k(T) = 1.66 \times 10^{15} \exp(-18748K/T)$ s$^{-1}$.

## References and Notes

(1) Melius, C. F. Thermochemical Modeling: I. Application to Decomposition of Energetic Materials. In *Chemistry and Physics of Energetics Materials*; Bulusu, S. N., Ed.; Kluwer Academic: Dordrecht, 1990.

(2) Belyayeva, M. S.; Klimenko, G. K.; Babaytseva, L. T.; Stolyarov, P. N. Fifth All Union Symposium on Combustion and Detonation, 1977.

(3) McMillen, D. F.; Barker, J. R.; Lewis, K. E.; Trevor, P. L.; Golden, D. M. "SRI Project PYU-5787", 1979.

(4) Maksimov, Y. Y.; Apol'kova, V. N.; Braverman, O. V.; Solov'en, A. I. *Russ. J. Phys. Chem.* **1985**, *59*, 9.

(5) Burov, Y. M.; Nazin, G. M. *Kinet. Catal.* **1982**, *23*, 5.

(6) Brill, T. B.; Gongwer, P. E.; Williams, G. K. *J. Phys. Chem.* **1994**, *98*, 12242.

(7) Smith, G. D.; Bharadwaj, R. K. *J. Phys. Chem. B* **1999**, *103*, 3570.

(8) Hariharan, P. C.; Koski, W. S.; Kaufman, J. J.; Miller, R. S.; Lowrey, H. A. *Int. J. Quantum Chem., Quantum Chem. Symp.* **1982**, *16*, 363.

(9) Politer, P.; Murray, J. S.; Lane, P. *Chem. Phys. Lett.* **1991**, *181*, 78.

(10) Kohno, Y.; Maekawa, K.; Tsuchioka, T.; Hashizume, T.; Imamura, A. *Combust. Flame* **1994**, *96*, 343.

(11) Rice, B. M.; Adams, G. F.; Page, M.; Thompson, D. L. *J. Phys. Chem.* **1995**, *99*, 5016.

(12) Johnson, M. A.; Truong, T. N. *J. Phys. Chem. A* **1999**, *103*, 8840.

(13) Truong, T. N. *J. Chem. Phys.* **1994**, *100*, 8014−8025.

(14) Duncan, W. T.; Bell, R. L.; Truong, T. N. *J. Comput. Chem.* **1998**, *19*, 1039−1052.

(15) Zhang, S.; Truong, T. N. *J. Comput. Chem.*

(16) Truhlar, D. G.; Garrett, B. C.; Klippenstein, S. J. *J. Phys. Chem.* **1996**, *100*, 12771.

(17) Hase, W. *Acc. Chem. Res.* **1998**, *31*, 659.

(18) Truong, T. N.; Duncan, W. T.; Bell, R. L. In *Chemical Applications of Density-Function Theory*; Brian, B. L., Ross, R. B., Ziegler, T., Eds.; American Chemistry Society: Washington, DC, 1996.

(19) Frisch, M. J.; Trucks, G. W.; Schlegel, H. B.; Scuseria, G. E.; Robb, M. A.; Cheeseman, J. R.; Zakrzewski, V. G.; Montgomery, J. J. A.; Stratmann, R. E.; Burant, J. C.; Dapprich, S.; Millam, J. M.; Daniels, A. D.; Kudin, K. N.; Strain, M. C.; Farkas, O.; Tomasi, J.; Barone, V.; Cossi, M.; Cammi, R.; Mennucci, B.; Pomelli, C.; Adamo, C.; Clifford, S.; Ochterski, J.; Petersson, G. A.; Ayala, P. Y.; Cui, Q.; Morokuma, K.; Malick, D. K.; Rabuck, A. D.; Raghavachari, K.; Foresman, J. B.; Cioslowski, J.; Ortiz, J. V.; Baboul, A. G.; Stefanov, B. B.; Liu, G.; Liashenko, A.; Piskorz, P.; Komaromi, I.; Gomperts, R.; Martin, R. L.; Fox, D. J.; Keith, T.; Al-Laham, M. A.; Peng, C. Y.; Nanayakkara, A.; Gonzalez, C.; Challacombe, M.; Gill, P. M. W.; Johnson, B.; Chen, W.; Wong, M. W.; Andres, J. L.; Gonzalez, C.; Head-Gordon, M.; Replogle, E. S.; Pople, J. A. *Gaussian 98*, Revision A.7; Gaussian, Inc.: Pittsburgh, PA, 1998.

(20) Cady, H. H.; Larson, A. C.; Cromer, D. T. *Acta Crystallogr.* **1963**, *16*, 617.

(21) Johnson, M. A.; Truong, T. N. *J. Phys. Chem. B* **1999**, *103*, 9392.

(22) Lide, D. R. *CRC Hand Book of Chemistry and Physics*, 80th ed.; CRC Press: Boca Raton, FL, 1999.